

# ZZγ and Zγγ couplings in γe collision with polarized beams

S. Atağ\* and İ. Şahin†

Department of Physics, Faculty of Sciences, Ankara University, 06100 Tandoğan, Ankara, Turkey

The potential of γe mode of linear e<sup>+</sup>e<sup>-</sup> collider to probe ZZγ and Zγγ vertices is investigated through the Z boson production from the process γe → Ze. Considering the longitudinal and transverse polarization states of the Z boson and incoming polarized beams we find the 95% C.L. limits on the form factors h<sub>3</sub><sup>Z</sup>, h<sub>4</sub><sup>Z</sup>, h<sub>3</sub><sup>γ</sup> and h<sub>4</sub><sup>γ</sup> with integrated luminosity 500 fb<sup>-1</sup> and √s = 0.5, 1, 1.5 TeV energies. It is shown that the polarization can improve sensitivities by factors 2-3 depending on the energy.

PACS numbers: 12.15.Ji, 12.15.-y, 12.60.Cn, 14.80.Cp

## I. INTRODUCTION

Studies of the trilinear gauge boson couplings provide important tests of the standard model (SM) of electroweak interactions. The SM predicts no tree-level couplings between the Z boson and the photon. Deviation of the couplings from the expected values would indicate the existence of new physics beyond the SM. Therefore precision measurements of triple vector boson vertices will be the crucial tests of the structure of the SM.

Possible anomalous ZZγ and Zγγ couplings must obey Lorentz and gauge invariance. Within the formalism of Ref. [1] there are eight anomalous coupling parameters h<sub>i</sub><sup>Z</sup>, h<sub>i</sub><sup>γ</sup> (i = 1, ..., 4) which are all zero in the standard model. Here we are interested in CP-even couplings that are proportional to h<sub>3</sub><sup>V</sup> and h<sub>4</sub><sup>V</sup> (V = Z, γ). Due to partial wave unitarity constraints at high energies, an energy dependent form factor ansatz can be considered:

$$h_i^V(\hat{s}) = \frac{h_{i0}^V}{(1 + \hat{s}/\Lambda^2)^3} \quad ; \quad i = 1, 3 \quad (1)$$

$$h_i^V(\hat{s}) = \frac{h_{i0}^V}{(1 + \hat{s}/\Lambda^2)^4} \quad ; \quad i = 2, 4 \quad (2)$$

In this work we assume that new physics scale Λ is above the collision energy √ŝ.

Therefore, CP conserving anomalous Z(p<sub>1</sub>)γ(p<sub>2</sub>)Z(p<sub>3</sub>) vertex function can be written following the papers of [1]:

$$ig_e \Gamma_{ZZ\gamma}^{\alpha\beta\mu}(p_1, p_2, p_3) = ig_e \frac{p_3^2 - p_1^2}{m_Z^2} \left[ h_3^Z \epsilon^{\mu\alpha\beta\rho} p_{2\rho} + \frac{h_4^Z}{m_Z^2} p_3^\alpha \epsilon^{\mu\beta\rho\sigma} p_{3\rho} p_{2\sigma} \right] \quad (3)$$

where m<sub>Z</sub> and g<sub>e</sub> are the Z-boson mass and charge of the proton. The Zγγ vertex function can be obtained with the replacements:

$$\frac{p_3^2 - p_1^2}{m_Z^2} \rightarrow \frac{p_3^2}{m_Z^2}, \quad h_i^Z \rightarrow h_i^\gamma, \quad i = 3, 4 \quad (4)$$

The overall factor p<sub>3</sub><sup>2</sup> in the Zγγ vertex function originates from electromagnetic gauge invariance. Due to Bose statistics the Zγγ vertex vanishes identically if both photons are on shell (Yang's theorem) [2].

Previous limits on the ZZγ and Zγγ anomalous couplings have been provided by the Tevatron |h<sub>3</sub><sup>Z</sup>| < 0.36, |h<sub>4</sub><sup>Z</sup>| < 0.05, |h<sub>3</sub><sup>γ</sup>| < 0.37 and |h<sub>4</sub><sup>γ</sup>| < 0.05 [3] and LEP experiments -0.50 < h<sub>3</sub><sup>Z</sup> < 0.36, -0.12 < h<sub>4</sub><sup>Z</sup> < 0.39, -0.33 < h<sub>3</sub><sup>γ</sup> < 0.01 and -0.02 < h<sub>4</sub><sup>γ</sup> < 0.24 [4] at 95% C.L. .

Based on the analysis of ZZ production at the upgraded Fermilab Tevatron and the CERN Large Hadron Collider (LHC) achievable limits on the ZZγ couplings have been discussed [5].

\*atag@science.ankara.edu.tr

†sahin@science.ankara.edu.tr

Research and development on linear  $e^+e^-$  colliders at SLAC, DESY and KEK have been progressing and the physics potential of these future machines is under intensive study. After linear colliders are constructed  $\gamma e$  and  $\gamma\gamma$  modes with real photons should be discussed and may work as complementary to basic colliders [6, 7]. Real gamma beam is obtained by the Compton backscattering of laser photons off linear electron beam where most of the photons are produced at the high energy region. Since the luminosities for  $\gamma e$  and  $\gamma\gamma$  collisions turn out to be of the same order as the one for  $e^+e^-$  collision [8], the cross sections for photoproduction processes with real photons are considerably larger than virtual photon case. Polarizability of real gamma beam is an additional advantage for polarized beam experiments. In this paper we examine the capability of  $\gamma e$  mode of LC to probe anomalous  $ZZ\gamma$  and  $Z\gamma\gamma$  couplings from Z boson production with polarized electron and gamma beams, assuming Z polarization will be measured.

## II. CROSS SECTIONS

For  $\gamma e \rightarrow Ze$  subprocess the helicity dependent differential cross section is given by

$$\begin{aligned} \frac{d\hat{\sigma}(\lambda_0, \lambda_Z)}{d\cos\theta} = & \frac{\beta}{32\pi\hat{s}} \left\{ \frac{1}{4}(1 - P_e) [(1 + \xi(\omega, \lambda_0)) |M(+, L; \lambda_Z, L)|^2 + (1 - \xi(\omega, \lambda_0)) |M(-, L; \lambda_Z, L)|^2] \right. \\ & \left. + \frac{1}{4}(1 + P_e) [(1 + \xi(\omega, \lambda_0)) |M(+, R; \lambda_Z, R)|^2 + (1 - \xi(\omega, \lambda_0)) |M(-, R; \lambda_Z, R)|^2] \right\} \end{aligned} \quad (5)$$

where  $\theta$  is the angle between incoming photon with helicity  $\lambda_\gamma$  and outgoing Z boson with helicity  $\lambda_Z$  in the c.m. frame. Helicity amplitudes  $M(\lambda_\gamma, \sigma_e; \lambda_Z, \sigma'_e)$  are given in the appendix.  $\sigma_e$  and  $\sigma'_e$  are incoming and outgoing electron helicities. Above cross section has been connected to initial laser photon helicity  $\lambda_0$  before Compton backscattering.  $P_e$  is the initial electron beam polarization and  $\xi(E_\gamma, \lambda_0)$  is the helicity of the Compton backscattered photon [8, 9]

$$\xi(E_\gamma, \lambda_0) = \frac{\lambda_0(1 - 2r)(1 - y + 1/(1 - y)) + \lambda_e r \zeta [1 + (1 - y)(1 - 2r)^2]}{1 - y + 1/(1 - y) - 4r(1 - r) - \lambda_e \lambda_0 r \zeta (2r - 1)(2 - y)} \quad (6)$$

Here  $r = y/[\zeta(1 - y)]$ ,  $y = E_\gamma/E_e$  and  $\zeta = 4E_e E_0/M_e^2$ .  $E_0$  is the energy of initial laser photon and  $E_e$  and  $\lambda_e$  are the energy and the helicity of initial electron beam before Compton backscattering. One should note that  $P_e$  and  $\lambda_e$  refer to different electron beams. In the cross section calculation we will keep  $\lambda_e = 0$  because of its minor contribution. The behaviour of the helicity of backscattered photons can be observed from Fig. 1 as a function of their energy. From the figure we see that the backscattered photons reach maximum polarization at highest energy region. For outgoing Z bosons we take into account the possibility that the transverse and longitudinal polarizations can be observed for each  $\lambda_0$  state.

The cross sections which will be used in our calculations are as follows

$$\frac{d\hat{\sigma}(\lambda_0, TR)}{d\cos\theta} = \frac{d\hat{\sigma}(\lambda_0, +)}{d\cos\theta} + \frac{d\hat{\sigma}(\lambda_0, -)}{d\cos\theta} \quad (7)$$

$$\frac{d\hat{\sigma}(\lambda_0, LO)}{d\cos\theta} = \frac{d\hat{\sigma}(\lambda_0, 0)}{d\cos\theta} \quad (8)$$

where TR stands for transverse and LO for longitudinal. For the unpolarized beams the cross section takes the form

$$\frac{d\hat{\sigma}^{unpol}}{d\cos\theta} = \frac{d\hat{\sigma}(\lambda_0, TR)}{d\cos\theta} + \frac{d\hat{\sigma}(\lambda_0, LO)}{d\cos\theta} \quad (9)$$

with  $\lambda_0 = 0$ ,  $\lambda_e = 0$  and  $P_e = 0$ .

For the integrated cross section, we need the spectrum of backscattered photons in connection with helicities of initial laser photon and electron which is given below [8, 9]

$$f_{\gamma/e}(y) = \frac{1}{g(\zeta)} \left[ 1 - y + \frac{1}{1 - y} - \frac{4y}{\zeta(1 - y)} + \frac{4y^2}{\zeta^2(1 - y)^2} + \lambda_0 \lambda_e r \zeta (1 - 2r)(2 - y) \right] \quad (10)$$

where

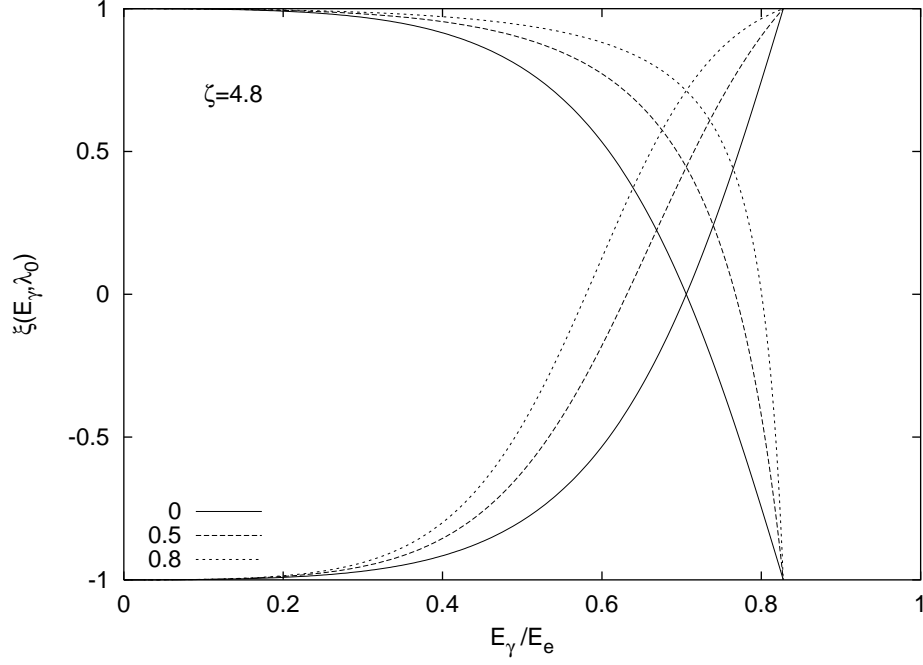


FIG. 1: Helicity of the backscattered photons as a function of their energy. The set of curves from the bottom (upper) are plotted for  $\lambda_0 = -1$  ( $\lambda_0 = 1$ ) and the legends are for helicities of the initial electron beam  $\lambda_e$ .

$$g(\zeta) = g_1(\zeta) + \lambda_0 \lambda_e g_2(\zeta)$$

$$g_1(\zeta) = \left(1 - \frac{4}{\zeta} - \frac{8}{\zeta^2}\right) \ln(\zeta + 1) + \frac{1}{2} + \frac{8}{\zeta} - \frac{1}{2(\zeta + 1)^2} \quad (11)$$

$$g_2(\zeta) = \left(1 + \frac{2}{\zeta}\right) \ln(\zeta + 1) - \frac{5}{2} + \frac{1}{\zeta + 1} - \frac{1}{2(\zeta + 1)^2} \quad (12)$$

The definitions of  $r$ ,  $y$  and  $\zeta$  are the same as in the helicity expression and the maximum value of  $y$  reaches 0.83 when  $\zeta = 4.8$ . To see the influence of polarization, energy distributions of backscattered photons  $f_{\gamma/e}$  is plotted for  $\lambda_0 \lambda_e = 0, -0.5, -0.8$  in Fig. 2.

The expression of the integrated cross section over the backscattered photon spectrum is written below for completeness:

$$\frac{d\sigma(\lambda_0, \lambda_Z)}{d \cos \theta} = \int_{y_{min}}^{0.83} f_{\gamma/e}(y) \frac{d\hat{\sigma}(\lambda_0, \lambda_Z)}{d \cos \theta} dy \quad (13)$$

with  $y_{min} = M_Z^2/s$ . Here  $\hat{s}$  is related to  $s$ , the square of the center of mass energy of  $e^+e^-$  system, by  $\hat{s} = ys$ .

In order to give an idea about the comparison of unpolarized and polarized cases, integrated total cross sections as functions of  $\sqrt{s}$  are shown in Figs. 3-5 for various coupling values and different configurations of polarizations. From figures we see global enhancement of the cross sections when anomalous contributions are included especially after  $\sqrt{s} \sim 1$  TeV region. Common feature in each figure is that higher  $\sqrt{s}$  will highly improve the sensitivity of the cross section to  $h_4^Z$  and  $h_4^\gamma$  when compared with  $h_3^Z$  and  $h_3^\gamma$ . Another important feature is the longitudinal polarization of Z boson which makes the separation much higher than the standard model. As can be seen from Fig. 1  $\xi(E_\gamma, \lambda_0)$  is antisymmetric with respect to  $\lambda_0$  when  $\lambda_e = 0$ . Thus, the contribution of the factor  $\xi(E_\gamma, \lambda_0)P_e$  to the cross section does not change by reversing the sign of both  $\lambda_0$  and  $P_e$ . This leads to the fact that we get almost the same plots as Figs. 4 and 5 if we reverse the sign of both  $\lambda_0$  and  $P_e$ . This feature also appears in the angular distributions below and on the tables of sensitivities in the next section. This is why we avoid to plot more figures.

It is also important to see how the anomalous couplings change the shape of the angular distribution of the Z boson for the polarized and unpolarized cases. We use the integrated cross section formula to obtain angular distributions in Figs. 6-8. Much larger deviations still arise from  $h_4^V$  for both TR and LO polarizations. The shape of the curves differs

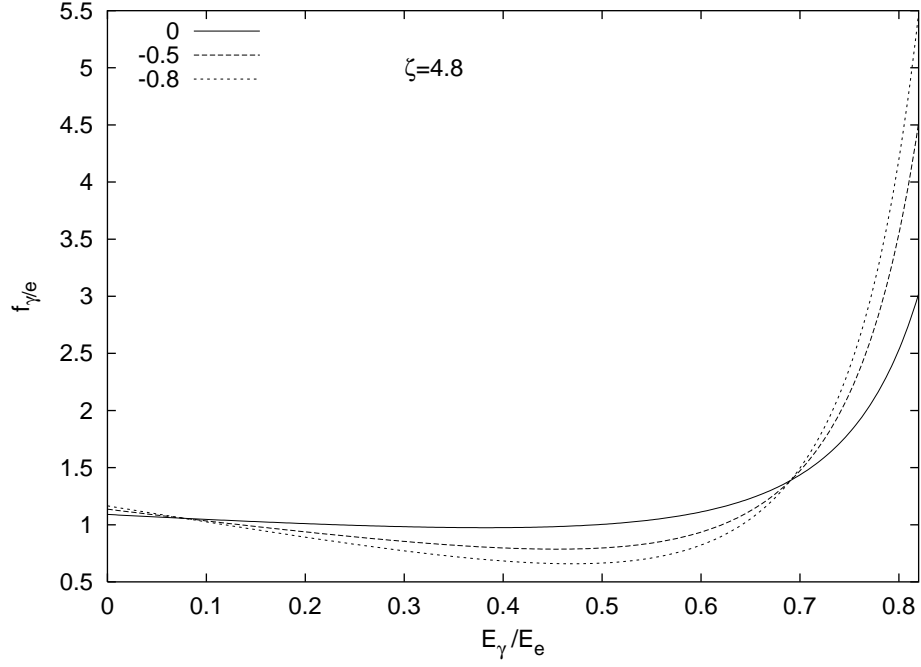


FIG. 2: Energy distribution of the backscattered photons for  $\lambda_0\lambda_e = 0, -0.5, -0.8$ .

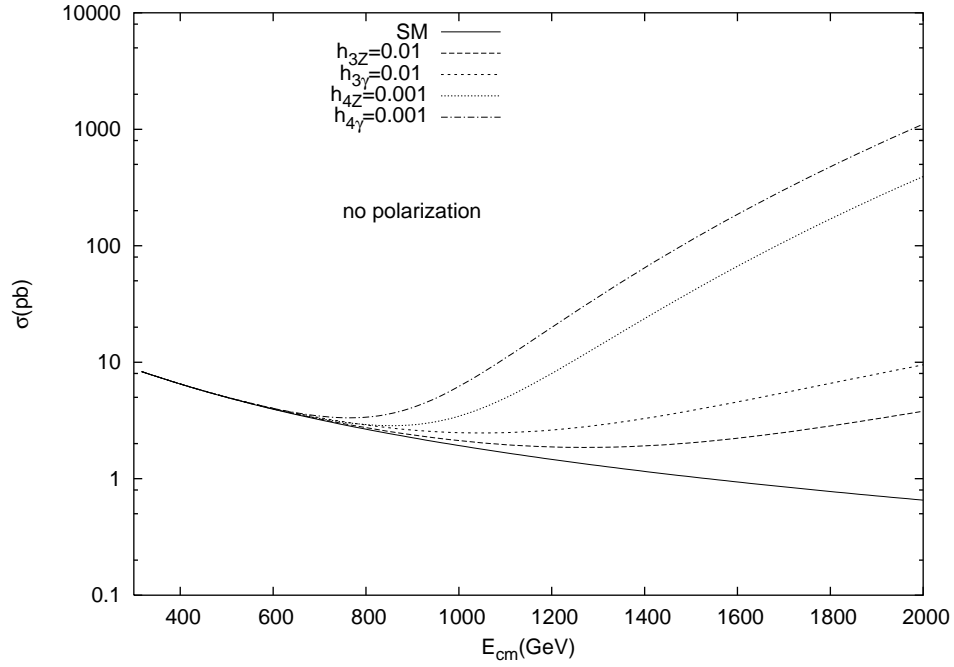


FIG. 3: Total cross section versus the center of mass energy  $\sqrt{s}$  of the parental linear  $e^+e^-$  colliders for the unpolarized case. CP conserving coupling parameters of  $ZZ\gamma$  and  $Z\gamma\gamma$  vertices are shown on the figure.

for two kinds of polarizations of the Z boson. Additionally,  $Z\gamma\gamma$  couplings always provide the higher contribution to the cross section than the  $ZZ\gamma$  couplings. Each time only one of the coupling parameters have been kept different from zero. Numerical results for all polarization configurations will be given in the next section.

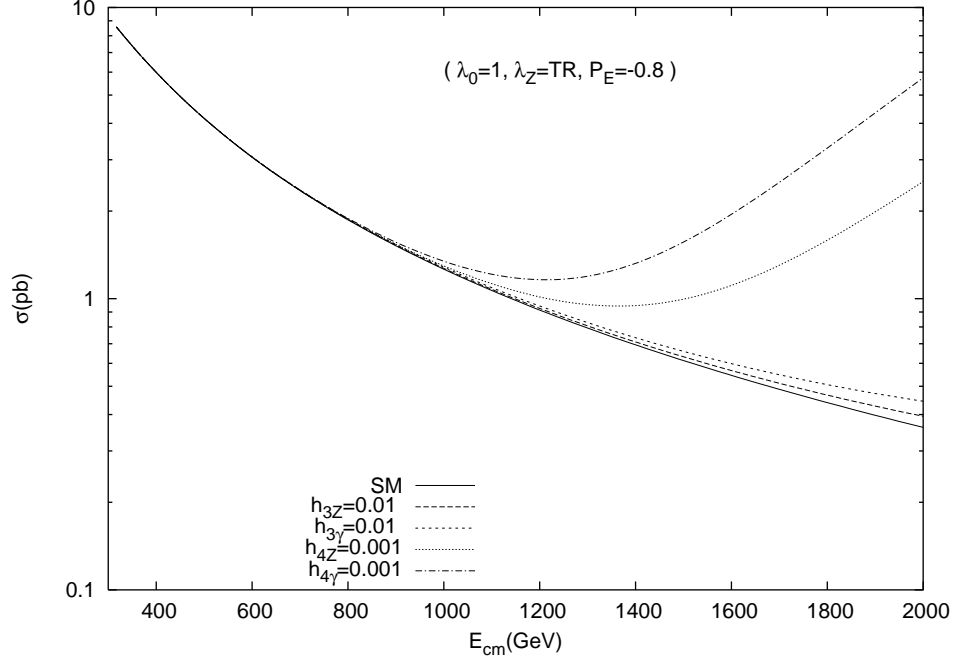


FIG. 4: The same as in Fig.3 but for polarization parameters  $\lambda_0 = 1$ ,  $\lambda_Z = TR$  and  $P_E = -0.8$ . TR and LO are for transverse and longitudinal polarization.

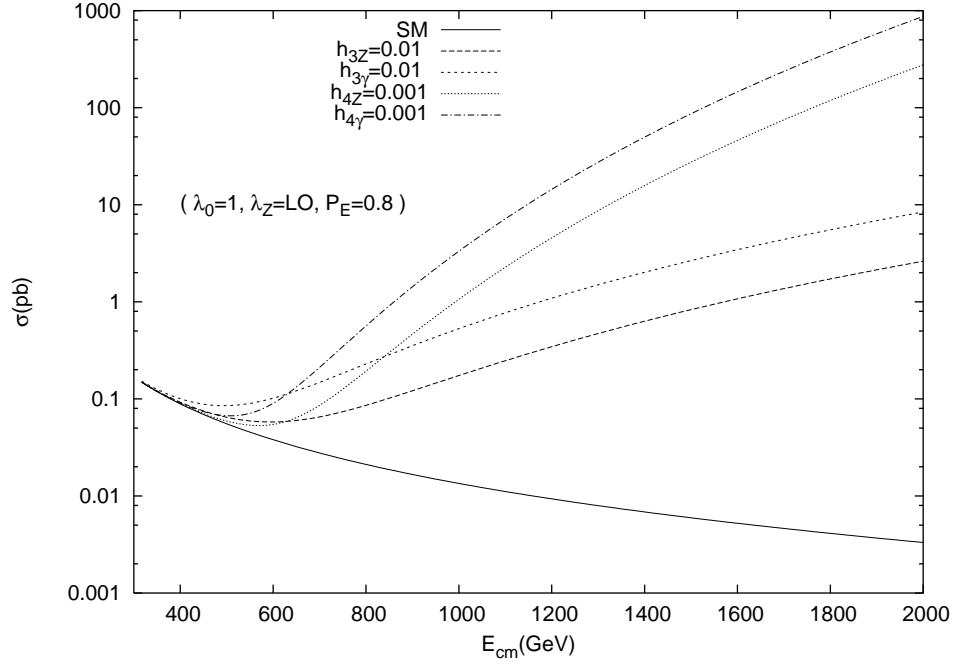


FIG. 5: The same as in Fig.3 but for polarization parameters  $\lambda_0 = 1$ ,  $\lambda_Z = LO$  and  $P_E = 0.8$ .

### III. LIMITS ON THE ANOMALOUS COUPLING PARAMETERS

In order to obtain realistic limits on the  $h_3^V$  and  $h_4^V$  from the LC-based  $\gamma e$  collider the number of events have been calculated using  $N = A\sigma(\gamma e \rightarrow Ze)Br(Z \rightarrow \ell^+\ell^-)L_{int}$  for integrated luminosity  $L_{int} = 500 fb^{-1}$ . Here lepton channel of the Z decay and overall acceptance  $A=0.65$  has been taken into account. For total cross section  $|\cos\theta| = 0.9$  has been used as angular region. The 95% confidence level (C.L.) limits have been estimated using simple one parameter

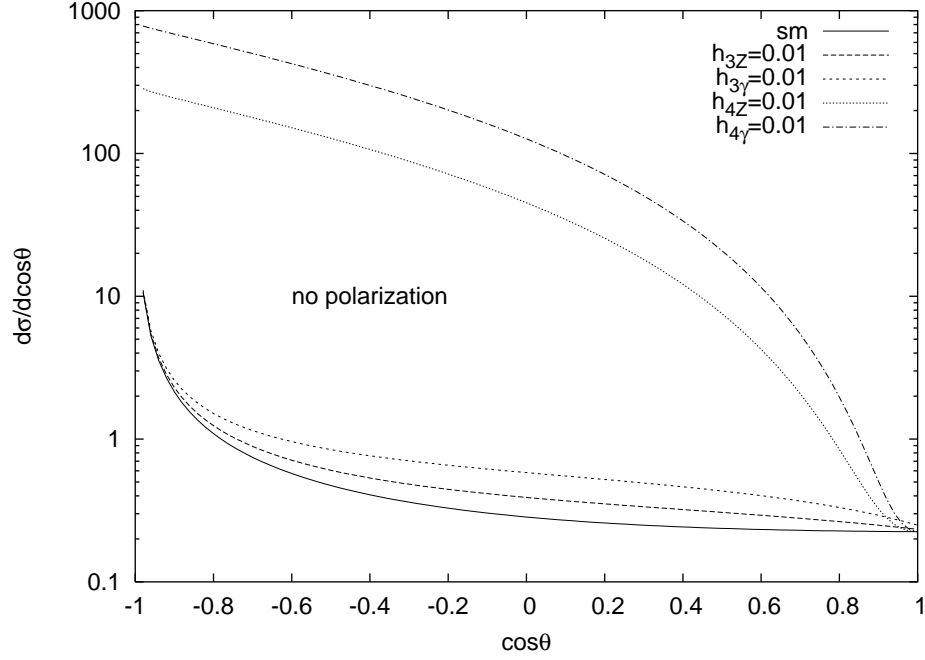


FIG. 6: Dependence of the angular distribution of the Z boson on the coupling parameters of  $ZZ\gamma$  and  $Z\gamma\gamma$  vertices for the unpolarized case. The unit of the cross section is pb.

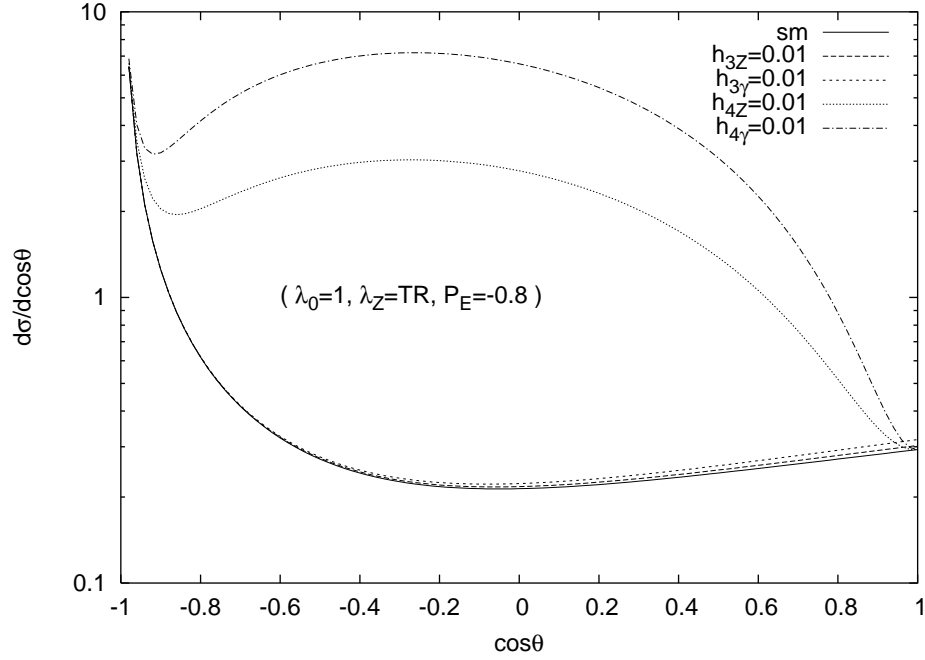


FIG. 7: The same as in Fig.6 but for the polarization parameters shown on the graph.

$\chi^2$  test for  $\sqrt{s} = 0.5, 1, 1.5$  TeV from total cross section. Angular distributions with binning procedure yield almost the same limits as that of total cross section. At least 200 or more events have been considered in all calculations. The limits which have been obtained are shown in Tables I-III for the deviation of the cross section from the standard model value without systematic error. It should be noted that better limits are obtained for the polarization configuration  $\lambda_0 = -1$ ,  $\lambda_Z = \text{LO}$  and  $P_e = -1$  which leads to the order of  $O(10^{-4})$  for  $h_3^Z$  and  $h_3^\gamma$ ,  $O(10^{-6})$  for  $h_4^Z$  and  $h_4^\gamma$  at  $\sqrt{s} = 1.5$  TeV. Polarization improves the limits on  $h_3^Z$  and  $h_4^Z$  by factors 2.5-3,  $h_3^\gamma$  by factors 2-2.5 and  $h_4^\gamma$  by factors

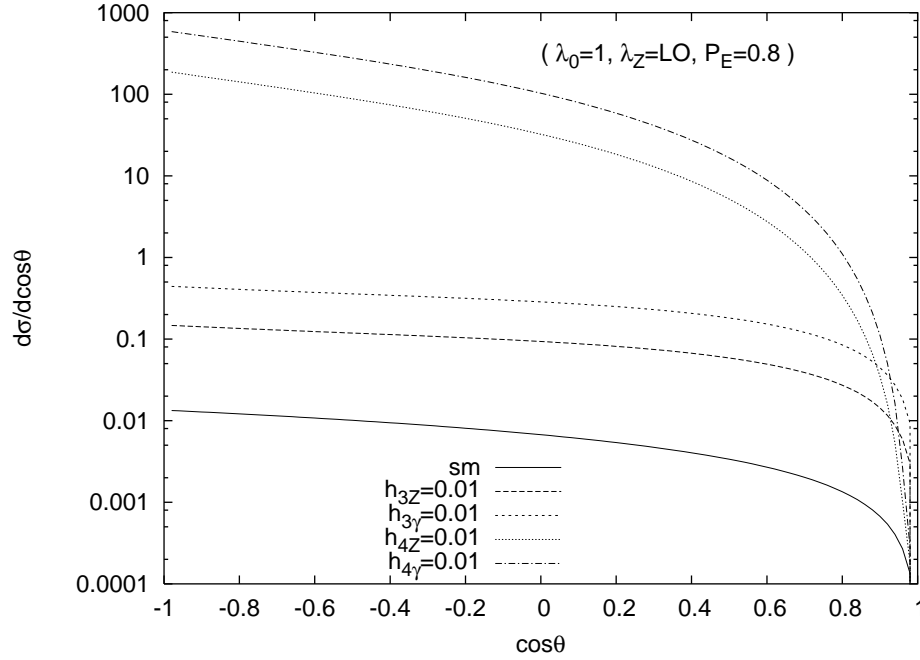


FIG. 8: The same as in Fig.6 but for the polarization parameters shown on the graph.

2-3 depending on energy for the case of the polarization configuration given above. In order to see the degree of energy dependence on the anomalous couplings let us take into account the increase in c.m. energy from 0.5 TeV to 1.5 TeV for the same polarization configuration. Then we get the improvements in sensitivity limits by a factor 10 for  $h_3^Z$ , by a factor 14 for  $h_3^\gamma$ , by a factor 170 for  $h_4^Z$  and  $h_4^\gamma$ .

#### IV. CONCLUSION

As the complementary collider, the  $\gamma e$  mode of linear collider with luminosity comparable to that in the collision  $e^+e^-$  probes the  $ZZ\gamma$  and  $Z\gamma\gamma$  anomalous couplings with far better sensitivity than the present colliders Fermilab Tevatron and LEP2 experiments. Predictions from CERN LHC [5] and parental linear  $e^+e^-$  collider [10] have been given for coupling parameters  $f_i^V$  ( $i = 4, 5$ ;  $V = Z, \gamma$ ) due to  $ZZ$  productions. Thus, one to one comparison with them is not possible.

In order to reach realistic results a few comments are in order. A reduction in luminosity is expected in the  $\gamma e$  collision when compared to the basic  $e^+e^-$  collision due to scattering of laser photons. However, there are some possibilities for increasing luminosity using electron beams with low emittances [11].

The Z boson polarization can be measured via lepton pair channel of the Z decay. Measurements of the helicity and the angular distribution of the final leptons are closely related Z boson polarization due to angular momentum conservation. An asymmetry measurement with polarized Z boson can be found in Ref. [12] to get more information.

The results presented in this paper are based on tree level analysis. One-loop electroweak corrections may introduce large logarithms as in the unpolarized total cross section. Furthermore, the helicity dependence of the one-loop amplitudes involving the exchange of Z boson is different from the tree-level form. This is the theoretical uncertainty that influences the systematic error.

Other than the theoretical uncertainty, expected sources of systematic errors may result from the uncertainty on the measurement of  $\gamma e$  luminosity, helicity of incoming photons after Compton backscattering and uncertainty on the photon spectra [13].

For more precise results, further analysis needs to be supplemented by observables such as the distributions of the Z decay products with a more detailed knowledge of the experimental conditions.

TABLE I: Sensitivity of the  $\gamma e$  collider to  $ZZ\gamma$  and  $Z\gamma\gamma$  couplings at 95% C.L. for  $\sqrt{s} = 0.5$  TeV and  $L_{int} = 500 \text{ fb}^{-1}$ . Only one of the couplings is assumed to deviate from the SM at a time.

$\lambda_0$	$\lambda_Z$	$P_e$	$h_3^Z(10^{-2})$	$h_4^Z(10^{-3})$	$h_3^\gamma(10^{-2})$	$h_4^\gamma(10^{-3})$
0	TR+LO	0	-1, 1	-2, 2	-0.7, 0.7	-1, 1
1	TR	-0.8	-3, 3	-5, 5	-2, 2	-3, 3
-1	TR	-0.8	-3, 3	-7, 7	-2, 2	-4, 4
1	LO	-0.8	-0.7, 0.7	-1, 1	-0.5, 0.5	-0.7, 0.7
-1	LO	-0.8	-0.4, 0.4	-0.8, 0.8	-0.3, 0.3	-0.5, 0.5
1	TR	0.8	-3, 3	-7, 7	-2, 2	-4, 4
-1	TR	0.8	-3, 3	-6, 6	-2, 2	-3, 3
1	LO	0.8	-0.5, 0.5	-0.9, 0.9	-0.3, 0.3	-0.5, 0.5
-1	LO	0.8	-0.8, 0.8	-1, 1	-0.4, 0.4	-0.6, 0.6

TABLE II: Sensitivity of the  $\gamma e$  collider to  $ZZ\gamma$  and  $Z\gamma\gamma$  couplings at 95% C.L. for  $\sqrt{s} = 1$  TeV and  $L_{int} = 500 \text{ fb}^{-1}$ . Only one of the couplings is assumed to deviate from the SM at a time.

$\lambda_0$	$\lambda_Z$	$P_e$	$h_3^Z(10^{-3})$	$h_4^Z(10^{-5})$	$h_3^\gamma(10^{-3})$	$h_4^\gamma(10^{-5})$
0	TR+LO	0	-2, 2	-9, 9	-1, 1	-5, 5
1	TR	-0.8	-10, 10	-50, 50	-7, 7	-30, 30
-1	TR	-0.8	-10, 10	-60, 60	-8, 8	-40, 40
1	LO	-0.8	-1, 1	-5, 5	-0.8, 0.8	-3, 3
-1	LO	-0.8	-0.7, 0.7	-3, 3	-0.5, 0.5	-2, 2
1	TR	0.8	-10, 10	-70, 70	-7, 7	-40, 40
-1	TR	0.8	-10, 10	-50, 50	-6, 6	-30, 30
1	LO	0.8	-0.9, 0.9	-4, 4	-0.5, 0.5	-2, 2
-1	LO	0.8	-1, 1	-5, 5	-0.8, 0.8	-3, 3

- 
- [1] U. Baur and E. L. Berger, Phys. Rev. **D47**, 4889 (1993);  
K. Hagiwara *et al.*, Nucl. Phys. **B282**, 253 (1987);  
F.M. Renard, Nucl. Phys. **B196**, 93 (1982).  
[2] C. N. Yang, Phys. Rev. **77**, 242 (1950).  
[3] D0 Collaboration, B. Abbott *et al.* Phys. Rev. **D57**, R3817 (1998);  
D0 Collaboration, S. Abachi *et al.* Phys. Rev. Lett. **75**, 1028 (1995);

TABLE III: Sensitivity of the  $\gamma e$  collider to  $ZZ\gamma$  and  $Z\gamma\gamma$  couplings at 95% C.L. for  $\sqrt{s} = 1.5$  TeV and  $L_{int} = 500 \text{ fb}^{-1}$ . Only one of the couplings is assumed to deviate from the SM at a time.

$\lambda_0$	$\lambda_Z$	$P_e$	$h_3^Z(10^{-4})$	$h_4^Z(10^{-5})$	$h_3^\gamma(10^{-4})$	$h_4^\gamma(10^{-5})$
0	TR+LO	0	-9, 9	-1, 1	-5, 5	-0.9, 0.9
1	TR	-0.8	-60, 60	-10, 10	-40, 40	-8, 8
-1	TR	-0.8	-70, 70	-20, 20	-40, 40	-10, 10
1	LO	-0.8	-5, 5	-0.7, 0.7	-3, 3	-0.5, 0.5
-1	LO	-0.8	-3, 3	-0.5, 0.5	-2, 2	-0.3, 0.3
1	TR	0.8	-70, 70	-20, 20	-40, 40	-10, 10
-1	TR	0.8	-60, 60	-10, 10	-30, 30	-7, 7
1	LO	0.8	-3, 3	-0.6, 0.6	-2, 2	-0.3, 0.3
-1	LO	0.8	-5, 5	-0.8, 0.8	-3, 3	-0.4, 0.4



- D0 Collaboration, S. Abachi *et al.* Phys. Rev. Lett. **78**, 3640 (1997).
- [4] L3 Collaboration, M. Acciarri *et al.*, Phys. Lett **B436**, 187 (1998);  
L3 Collaboration, M. Acciarri *et al.*, Phys. Lett **B346**, 190 (1995);  
DELPHI Collaboration, P. Abreu *et al.*, Phys. Lett. **B380**, 471 (1996).
- [5] U. Baur and D. Rainwater, Int. J. Mod. Phys. **A16S1A**, 315 (2001);  
U. Baur and D. Rainwater, Phys. Rev. **D62**, 113011 (2000).
- [6] C. Akerlof, Ann Arbor preprint UM HE 81-59 (1981).
- [7] T.L. Barklow, Proc. 1990 Summer Study on Research Directions for the Decade (Snowmass, CO, Jun-July 1990), and preprint SLAC-PUB-5364 (1990).
- [8] I.F. Ginzburg *et al.*, Nucl. Instrum. Methods **205**, 47 (1983); *ibid.* 219, 5 (1984).
- [9] V.I. Telnov, Nucl. Instrum. Methods **A294**, 72 (1990);  
D.I. Borden, D.A. Bauer and D.O. Caldwell, SLAC preprint SLAC-PUB-5715, Stanford (1992).
- [10] S. Rosati, talk given at Linear Collider Workshop, Padova, Italy, May 2000.
- [11] V. Telnov, Turk. J. Phys. **22**, 541 (1998).
- [12] SLD Collaboration, K. Abe *et al.*, Phys. Rev. Lett. **86** 1162 (2001); SLD Collaboration, K. Abe *et al.*, Phys. Rev. Lett. **79** 804 (1997).
- [13] V. Telnov, ECFA workshop, Amsterdam, April 1-4, 2003; PHOTON2003, Frascati, April 7-11, 2003;  
<http://www.ipp.dur.ac.uk/~gudrid/power/>.

## APPENDIX: HELICITY AMPLITUDES

There are four Feynman diagrams for the process  $\gamma e \rightarrow Ze$  if one includes  $ZZ\gamma$ ,  $Z\gamma\gamma$  vertices. Helicity amplitudes  $M_1$  and  $M_4$  are responsible for the diagrams concerning  $ZZ\gamma$  and  $Z\gamma\gamma$  interactions arising from t channel Z or  $\gamma$  exchanges.  $M_2$  and  $M_3$  are standard model contribution of the u and s channel of the process. The parameters of the helicity amplitudes  $M(\lambda_\gamma, \sigma_e; \lambda_Z, \sigma'_e)$  are helicities of incoming photon and electron, outgoing Z boson and electron. The values they take are given by :

$$\lambda_\gamma : +, - \quad , \quad \sigma_e : L, R \quad , \quad \lambda_Z : +, -, 0 \quad , \quad \sigma'_e : L, R \quad (A.1)$$

Here L and R stand for left and right. Helicity amplitudes we have obtained for each Feynman diagram in the c.m. frame of  $\gamma e$  can be written as follows:

$$\begin{aligned} M(\lambda_\gamma, \sigma_e; \lambda_Z, \sigma'_e) &= M_1(\lambda_\gamma, \sigma_e; \lambda_Z, \sigma'_e) + M_2(\lambda_\gamma, \sigma_e; \lambda_Z, \sigma'_e) \\ &+ M_3(\lambda_\gamma, \sigma_e; \lambda_Z, \sigma'_e) + M_4(\lambda_\gamma, \sigma_e; \lambda_Z, \sigma'_e) \end{aligned} \quad (A.2)$$

$$M_1(+L; +L) = C_1^L \left\{ h_3^Z \left[ iE_1 \left( \sin \theta \sin \frac{\theta}{2} - 2 \cos \frac{\theta}{2} \right) \right] + \frac{h_4^Z}{M_Z^2} \left[ -iE_1^2 p_3 (1 + \cos \theta) \sin \frac{\theta}{2} \sin \theta \right] \right\} \quad (\text{A.3})$$

$$M_1(+L; -L) = C_1^L \left\{ h_3^Z \left[ -iE_1 \sin \frac{\theta}{2} \sin \theta \right] + \frac{h_4^Z}{M_Z^2} \left[ ip_3 E_1^2 \cos \frac{\theta}{2} \sin^2 \theta \right] \right\} \quad (\text{A.4})$$

$$M_1(+L; 0L) = C_1^L \frac{\sqrt{2}}{M_Z} \left\{ h_3^Z \left[ iE_1 E_3 (1 + \cos \theta) \sin \frac{\theta}{2} \right] + \frac{h_4^Z}{M_Z^2} \left[ ip_3 E_1^2 \sin \frac{\theta}{2} (p_3 - E_3 \cos \theta) (1 + \cos \theta) \right] \right\} \quad (\text{A.5})$$

$$M_1(-L; +L) = C_1^L \left\{ \frac{h_4^Z}{M_Z^2} \left[ -iE_1^2 (p_3 + E_3) \sin \frac{\theta}{2} \sin \theta \right] \right\} \quad (\text{A.6})$$

$$M_1(-L; 0L) = C_1^L \frac{\sqrt{2}}{M_Z} \left\{ h_3^Z \left[ iE_1 (p_3 + E_3) \sin \frac{\theta}{2} \right] + \frac{h_4^Z}{M_Z^2} \left[ iE_1^2 \sin \frac{\theta}{2} (p_3^2 + E_3 p_3 (1 - \cos \theta) - E_3^2 \cos \theta) \right] \right\} \quad (\text{A.7})$$

$$M_1(-L; -L) = C_1^L \left\{ h_3^Z \left[ 2iE_1 \cos \frac{\theta}{2} \right] + \frac{h_4^Z}{M_Z^2} \left[ iE_1^2 (p_3 + E_3) \sin \frac{\theta}{2} \sin \theta \right] \right\} \quad (\text{A.8})$$

$$M_1(+R; +R) = C_1^R \left\{ h_3^Z \left[ -2iE_1 \cos \frac{\theta}{2} \right] + \frac{h_4^Z}{M_Z^2} \left[ -iE_1^2 (p_3 + E_3) \sin \frac{\theta}{2} \sin \theta \right] \right\} \quad (\text{A.9})$$

$$M_1(+R; -R) = C_1^R \left\{ \frac{h_4^Z}{M_Z^2} \left[ iE_1^2 (p_3 + E_3) \sin \frac{\theta}{2} \sin \theta \right] \right\} \quad (\text{A.10})$$

$$M_1(+R; 0R) = C_1^R \frac{\sqrt{2}}{M_Z} \left\{ h_3^Z \left[ iE_1 (p_3 + E_3) \sin \frac{\theta}{2} \right] + \frac{h_4^Z}{M_Z^2} \left[ iE_1^2 \sin \frac{\theta}{2} (p_3^2 + E_3 p_3 (1 - \cos \theta) - E_3^2 \cos \theta) \right] \right\} \quad (\text{A.11})$$

$$M_1(-R; +R) = C_1^R \left\{ h_3^Z \left[ iE_1 \sin \frac{\theta}{2} \sin \theta \right] + \frac{h_4^Z}{M_Z^2} \left[ -iE_1^2 p_3 (1 + \cos \theta) \sin \frac{\theta}{2} \sin \theta \right] \right\} \quad (\text{A.12})$$

$$M_1(-R; -R) = C_1^R \left\{ h_3^Z \left[ iE_1 \cos \frac{\theta}{2} (1 + \cos \theta) \right] + \frac{h_4^Z}{M_Z^2} \left[ iE_1^2 p_3 (1 + \cos \theta) \sin \frac{\theta}{2} \sin \theta \right] \right\} \quad (\text{A.13})$$

$$M_1(-R; 0R) = C_1^R \frac{\sqrt{2}}{M_Z} \left\{ h_3^Z \left[ iE_1 E_3 (1 + \cos \theta) \sin \frac{\theta}{2} \right] + \frac{h_4^Z}{M_Z^2} \left[ iE_1^2 p_3 \sin \frac{\theta}{2} (1 + \cos \theta) (p_3 - E_3 \cos \theta) \right] \right\} \quad (\text{A.14})$$

where

$$C_1^L = -\frac{2g_e g_L \sqrt{E_2 E_4}}{M_Z^2}, \quad C_1^R = -\frac{2g_e g_R \sqrt{E_2 E_4}}{M_Z^2} \quad (\text{A.15})$$

with

$$g_L = \frac{g_Z}{2} (C_V + C_A), \quad g_R = \frac{g_Z}{2} (C_V - C_A) \quad (\text{A.16})$$

$$C_V = 2 \sin^2 \theta_W - \frac{1}{2}, \quad C_A = -\frac{1}{2} \quad (\text{A.17})$$

$$g_Z = \frac{g_e}{\sin \theta_W \cos \theta_W}, \quad g_e^2 = 4\pi\alpha \quad (\text{A.18})$$

Here  $E_1$ : energy of incoming photon,  $E_2$ : energy of incoming electron,  $E_3$ : energy of outgoing Z boson,  $p_3 = |\vec{p}_3|$ : magnitude of the outgoing Z boson momentum,  $E_4$ : energy of outgoing electron.

$$M_2(+L; +L) = C_2^L \left\{ -(p_3 + E_3)(1 + \cos \theta) \cos \frac{\theta}{2} \right\} \quad (\text{A.19})$$

$$M_2(+L; -L) = C_2^L \left\{ (p_3 - E_3)(1 - \cos \theta) \cos \frac{\theta}{2} \right\} \quad (\text{A.20})$$

$$M_2(+L; 0L) = C_2^L \left\{ \sqrt{2} M_Z \sin \theta \cos \frac{\theta}{2} \right\} \quad (\text{A.21})$$

$$M_2(-L; +L) = C_2^L \left\{ (2E_1 - p_3 - E_3) \sin \theta \sin \frac{\theta}{2} \right\} \quad (\text{A.22})$$

$$M_2(-L; -L) = C_2^L \left\{ (E_3 - p_3 - 2E_1) \sin \theta \sin \frac{\theta}{2} \right\} \quad (\text{A.23})$$

$$M_2(-L; 0L) = C_2^L \frac{\sqrt{2}}{M_Z} \left\{ [(2E_1 E_3 - M_Z^2) \cos \theta + 2E_1 p_3] \sin \frac{\theta}{2} \right\} \quad (\text{A.24})$$

$$M_2(+R; +R) = C_2^R \left\{ (E_3 - p_3 - 2E_1) \sin \theta \sin \frac{\theta}{2} \right\} \quad (\text{A.25})$$

$$M_2(+R; -R) = C_2^R \left\{ (2E_1 - E_3 - p_3) \sin \theta \sin \frac{\theta}{2} \right\} \quad (\text{A.26})$$

$$M_2(+R; 0R) = C_2^R \frac{\sqrt{2}}{M_Z} \left\{ [(M_Z^2 - 2E_1 E_3) \cos \theta - 2E_1 p_3] \sin \frac{\theta}{2} \right\} \quad (\text{A.27})$$

$$M_2(-R; +R) = C_2^R \left\{ (p_3 - E_3)(1 - \cos \theta) \cos \frac{\theta}{2} \right\} \quad (\text{A.28})$$

$$M_2(-R; -R) = C_2^R \left\{ -(p_3 + E_3)(1 + \cos \theta) \cos \frac{\theta}{2} \right\} \quad (\text{A.29})$$

$$M_2(-R; 0R) = C_2^R \left\{ -\sqrt{2} M_Z \sin \theta \cos \frac{\theta}{2} \right\} \quad (\text{A.30})$$

where

$$C_2^L = \frac{2Q_e g_e g_L \sqrt{E_2 E_4}}{\hat{u} - M_e^2}, \quad C_2^R = \frac{2Q_e g_e g_R \sqrt{E_2 E_4}}{\hat{u} - M_e^2} \quad (\text{A.31})$$

$$\hat{u} = M_Z^2 - 2E_2(E_3 + p_3 \cos \theta), \quad Q_e = -1 \quad (\text{A.32})$$

$$M_3(+L; +L) = 0, \quad M_3(+L; -L) = 0 \quad (\text{A.33})$$

$$M_3(+L; 0L) = 0, \quad M_3(-L; +L) = 0 \quad (\text{A.34})$$

$$M_3(-L; -L) = C_3^L \left\{ 4E_1 \cos \frac{\theta}{2} \right\} \quad (\text{A.35})$$

$$M_3(-L; 0L) = C_3^L \frac{\sqrt{2}}{M_Z} \left\{ 2E_1(p_3 + E_3) \sin \frac{\theta}{2} \right\} \quad (\text{A.36})$$

$$M_3(+R; +R) = C_3^R \left\{ 4E_1 \cos \frac{\theta}{2} \right\} \quad (\text{A.37})$$

$$M_3(+R; -R) = 0 \quad (\text{A.38})$$

$$M_3(+R; 0R) = C_3^R \frac{\sqrt{2}}{M_Z} \left\{ -2E_1(p_3 + E_3) \sin \frac{\theta}{2} \right\} \quad (\text{A.39})$$

$$M_3(-R; +R) = 0, \quad M_3(-R; -R) = 0 \quad (\text{A.40})$$

$$M_3(-R; 0R) = 0 \quad (\text{A.41})$$

where

$$C_3^L = \frac{2Q_e g_e g_L \sqrt{E_2 E_4}}{\hat{s} - M_e^2}, \quad C_3^R = \frac{2Q_e g_e g_R \sqrt{E_2 E_4}}{\hat{s} - M_e^2} \quad (\text{A.42})$$

$$M_4(\lambda_\gamma, L; \lambda_Z, L) = C_4^L \left( \frac{1}{C_1^L} M_1(\lambda_\gamma, L; \lambda_Z, L) \right) \quad (\text{A.43})$$

$$M_4(\lambda_\gamma, R; \lambda_Z, R) = C_4^R \left( \frac{1}{C_1^R} M_1(\lambda_\gamma, R; \lambda_Z, R) \right) \quad (\text{A.44})$$

$$h_3^Z \rightarrow h_3^\gamma, \quad h_4^Z \rightarrow h_4^\gamma \quad (\text{A.45})$$

where

$$C_4^L = C_4^R = -\frac{2Q_e g_e^2 \sqrt{E_2 E_4}}{M_Z^2} \quad (\text{A.46})$$